- Technical Paper -

INFLUENCE OF GIRDER DETAILING ON THE SEISMIC BEHAVIOR OF H-SHAPED WALL STRUCTURE BY FINITE ELEMENT ANALYSIS

Jiehui WANG[*1], Koichi KUSUNOKI[*2]

ABSTRACT
In Japan, the concept of out-of-plane effective length has been defined and explained because of its contribution as an important parameter for the good seismic performance of wall structures. This study thus aims at the experimental test along with numerical investigation on the relationship between effective length and lateral deformation to understand the effective length expanding rule in wall structures with girder. The different roles of girder as the beam member or wall member based on different height of girder are also discussed and verified in this study.
Keywords: wall structure, girder, finite element analysis, effective length, out-of-plane wall

1. INTRODUCTION

Wall reinforced concrete structure (dubbed as WRC structure in this paper), which is one of the popular structural systems for residential buildings in Japan and some other countries, experiences mainly a lateral force when an earthquake is happening. This WRC structure consisting of bearing wall, out-of-plane wall and beam member demonstrates good seismic performance in some earthquakes. It has been clearly observed that WRC structures can remain without serious damages after some large earthquakes, such as Niigata earthquake in 1964, Tokachi-Oki earthquake in1968, Tohoku earthquake in 2011 and the Kumamoto earthquake in 2016. Then, several studies have been conducted to investigate the mechanism and behavior of this type of structure, including some static experiments and theoretical analysis on WRC structures under lateral force.

WRC structure is designed according to the Standard for Structural Design of Reinforced Concrete Boxed-shaped Wall Structures by Architectural Institute of Japan (dubbed as WRC standard in this paper) [1], in which the effective length of out-of-plane wall (dubbed as effective length hereinafter) which has been proved to be an important dominant factor for the good seismic performance of WRC structures. Besides, the effective length should be considered as the smaller value of six times the thickness of the adjacent bearing wall and a quarter of the span [1].

The effective length of out-of-plane wall in this work, has been identified as the following method shown in Fig.1: connecting all strength value of reinforcing bars to get area S2, which get the effective length from S1 which has the same area value with area S2.

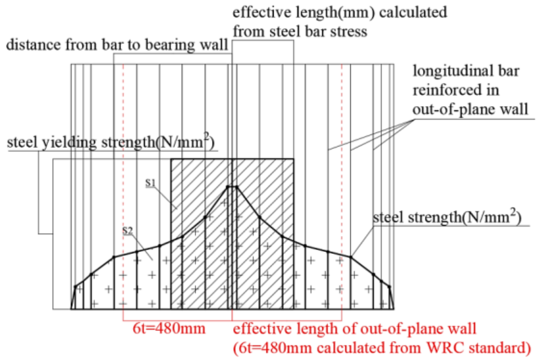

Fig.1 Calculating method of effective length

In previous studies, the effect of the out-of-plane wall has been well investigated in terms of seismic performance of WRC structures under experimental and analytical conditions. Based on these researches, the effective length calculated according to the WRC standard has been demonstrated to have a positive effect on the seismic performance of the whole WRC structure which has been extensively used in the design practice. Previous works on investigating the effective length have been conducted using simplified approaches with the cyclic loading experiment [2]. Researchers have studied the effective length of WRC walls with flexural yielding by cyclic loading experiment by conducting a wall structure with an out-of-plane wall designed after WRC standard to figure out the effective length around the elastic range. As mentioned before, previous research on investigating the performance of out-of-plane wall in WRC structural systems such as the deformation, cracks, and stiffness of out-of-plane wall, have been conducted using experiment and simulation methods.

*1 School of Engineering, The University of Tokyo, JCI Student Member
*2 Earthquake Research Institute, The University of Tokyo, JCI Member

However, there is still one issue need to be clarified related to the relationship between effective length and lateral deformation until the ultimate destruction stage for the whole structure: How does effective length expand under specified parameter of WRC structures.

This study thus aims to perform both experimental and numerical investigation on WRC structure to identify the relationship between effective length and lateral deformation until the ultimate destruction stage by presenting a WRC structure specimen and a corresponding simulation. The simulated response agrees well with the results of an experimental test conducted by Nagoya University under cyclic loadings on the WRC specimen [3]. Considering that the accuracy, stability, and reliability of the simulation model has been proved to be acceptable, the corresponding simulation concept composed of material models and modeling concept can be chosen to conduct a new model with girder in the bearing wall to figure out if the girder's height can bring difference on the changing law of out-of-plane wall's effective length.

2. BRIEF INTRODUCTION OF WALL TEST

2.1 Specimen introduction

1/2.5-scaled WRC structure specimen called 1NH is adopted in the experiment [3] to precisely reveal the behavior of the real structure with the space limitation of the strong reaction wall having been considered. The configuration of the abovementioned specimen 1NH is shown in Fig.2. The properties of steel bars and concrete are summarized in Table 1 and Table 2, respectively. Besides, the dimensions and reinforcement details of the scaled specimen 1NH are presented in Table 3. To study the influence of out-of-plane wall on the bearing capacity, a structural gap is set up between the out-of-plane wall and loading device to make sure that long-term loading would not apply to the out-of-plane directly and not bring any extra differences which can influence the effective length of the out-of-plane wall.

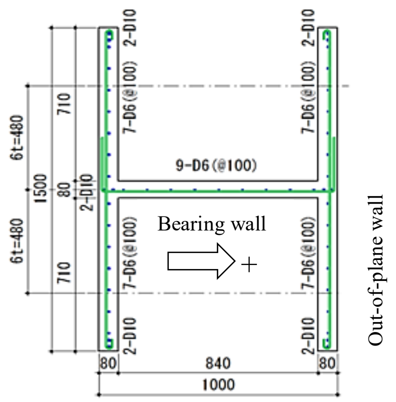

Fig.2 Configuration of specimen 1NH [3]

Table 1 Characteristics of steel bars

Type	Elastic Modulus	Yield strength	Yield strain	Tensile strength
	(kN/mm^2)	(N/mm^2)		(kN/mm^2)
D6	182	333	1850	492
D10	191	342	1795	495

Table 2 Characteristics of concrete

specimen	Elastic Modulus	Compressive strength	Tensile strength
	(kN/mm^2)	(N/mm^2)	(kN/mm^2)
1NH	252	27	2.19

Table 3 Characteristics of specimen

Bearing wall	width(mm) *thickness (mm)	1000 *80
	longitudinal reinforcement	9-D6@100
	lateral reinforcement	D6@100
	end reinforcement	2-D10
Out-of-plane wall	width(mm) *thickness (mm)	710 *80
	longitudinal reinforcement	7-D6@100
	lateral reinforcement	D6@100
	end reinforcement	2-D10

2.2 Loading Method

The loading device for this experiment is shown in Fig.3, where the constant vertical loads of 135kN are applied downward by two vertical actuators and cyclic lateral loads are applied by one horizontal actuator to conduct a cyclic static experiment. The vertical load applied to the two hydraulic jacks includes the 135kN that will be applied to the specimen and extra vertical force to make the inflection point just in the middle of the slab of the specimen.

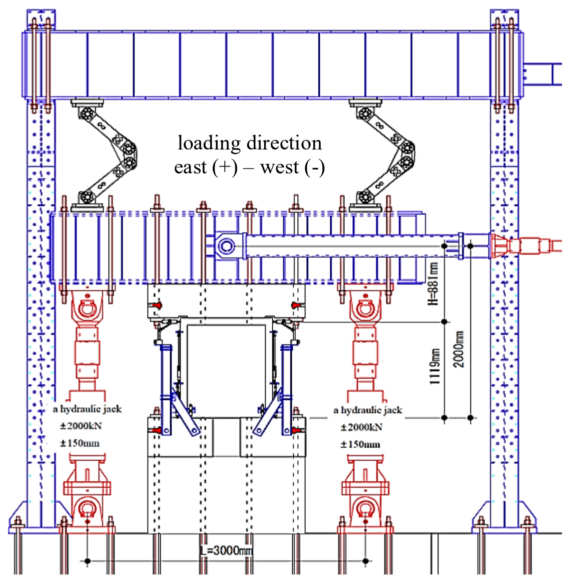

Fig.3 Loading equipment

2.3 Results of wall test

The lateral force-deformation curve of specimen 1NH derived from test [3] is presented in Fig.4. When the structure experiences a deformation of +1/610 rad and -1/420 rad, the lateral reinforcing bars of bearing wall yields (point A in Fig.4), and then the vertical reinforcing bars just beside bearing wall of out-of-plane wall yields (point B in Fig.4). When the structure experiences a deformation of +1/240 rad and -1/120 rad, the vertical reinforcing bars in bearing wall edge yields (point C in Fig.4). Next, when the deformation angle approaches ±1/100 rad, the vertical reinforcing bars in bearing wall intermediate portion yields (point D in Fig.4). Finally, when the deformation angle reaches ±1/77 rad, the maximum value of lateral bearing capacity is observed (point E in Fig.4).

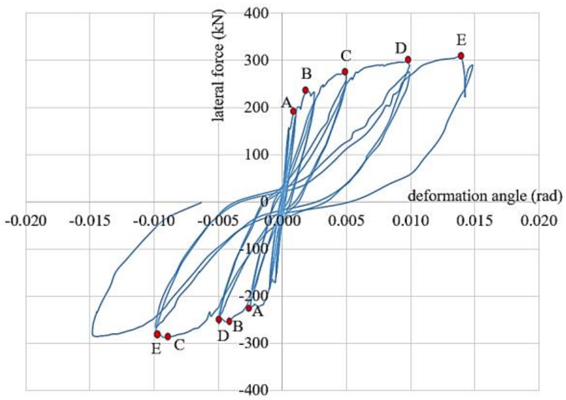

Fig.4 Force-deformation curve of test [3]

3. FEM SIMULATION OF WALL TEST

3.1 Model development

In this study, FEM analysis is adopted, and the configuration of model is set same as the design in the experiment mentioned above. The models of concrete and reinforcing steel are simulated with hexahedron element and truss element, respectively.

The hexahedron element for concrete consists of 8 points for each mesh is as shown in Fig.5. The concrete material utilized Naganuma・Yamakuchi model [4] for the concrete on the tensile side; modified Ahmad model for the ascending branch of the compressive stress-strain relationship [5]; modified Ahmad model for the property of concrete compression softening [5] and Fig.6 shows the modeled cyclic stress-strain relationship of concrete under tensile and compression developed by Naganuma・Okubo [6].

For the modeling of reinforcement steels, a tri-linear steel model is used in this analysis. The tri-linear steel model simulates the following characteristics of reinforcing bars: (1) elastic branch till yielding point and hardening branch with a strain-hardening ratio of 0.01 as shown in Fig.7; (2) kinematic strain hardening rule which considers the Baushinger effects consisting of (A) a descending of yielding stress in the tensile part while an ascending with the same value of yielding stress in the compressive part to keep the difference between tensile yielding stress and compressive yielding stress always constant and (B) decreasing of the curvature in the

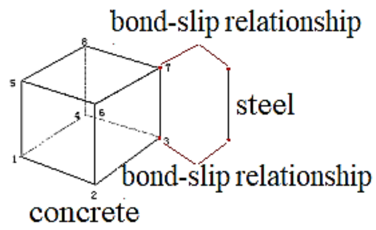

Fig.5 Hexahedron element for concrete and truss element for steel bar

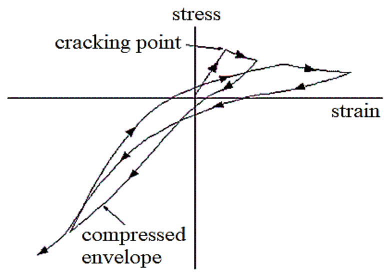

Fig.6 Cyclic stress-strain relationship of concrete

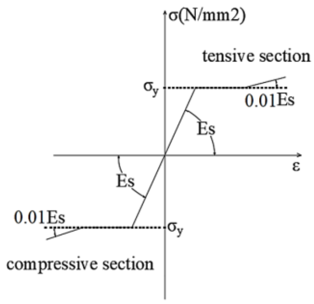

Fig.7 Tri-linear steel model

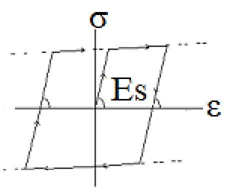

Fig.8 Kinematic strain hardening rule

transition zone and elastic to the plastic branches as shown in Fig.8.

Next, because the pull-out behavior has been considered for the reinforcing bars in wall elements, the bond-slip deformation in the reinforced concrete model [7] is conducted as shown in Fig.9. The maximum bond stress τ_u is calculated based on the WRC standard [1]. Furthermore, the loading condition of the simulation is the same as that in the experimental test,

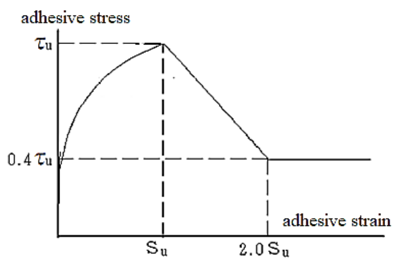

Fig.9 Bond-slip relationship

and the walls are fixed on the ground. Finally, the FEM model adopted in the simulation is depicted as Fig.10.

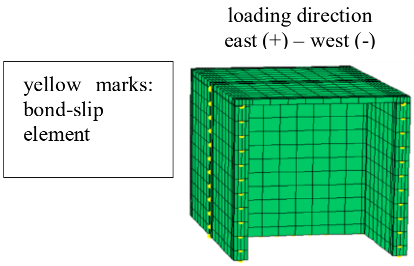

Fig.10 Model 1NH of simulation

3.2 Comparison between simulation and test

The comparison between the experimental and simulation results are shown in Fig.11.

It is found that a good agreement has been established in this correlation before 1/400 rad, but after 1/400 rad, the strength of simulation is descending which cannot be captured in the experimental result. For this disagreement, the severe cracking or considerable strength loss of concrete under a cyclic loading is considered as the main reason why the strength of simulation descending after 1/400 rad. Furthermore, the modeling method of this simulation can be applied for further simulations to discuss some other analysis towards the strength of the whole wall by 1/400 rad which has been validated to be reliable, and only discussing the fundamental tendency of effective length of out-of-plane wall up to 1/100 rad which shows a little disagreement with experimental test.

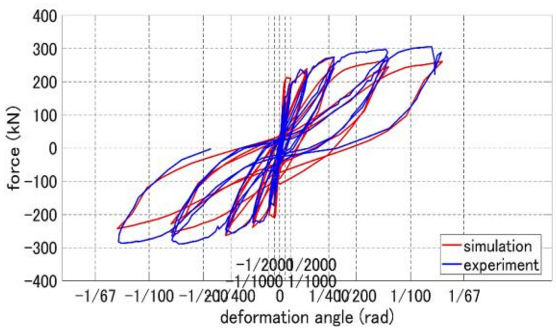

Fig.11 Comparison of force-deformation curves

4. SIMULATION OF MODEL WITH GIRDER

As mentioned in the former section, the modeling concept can be adopted for further analysis. And the simulation applied in this section are up to 1/100 rad that the validity of the model has been confirmed in section 3. When applying a wall structure with an opening as shown in Fig.12, in which two bearing walls are connected by a girder with height of h mm, the whole strength calculated based on WRC standard [1] would be the same regardless of the height of girder. That is because, based on the calculating equation for wall strength, when the length of the whole bearing wall including openings between out-of-plane walls keeps at the same value, the height of the girder is not an effective parameter for the strength of whole wall

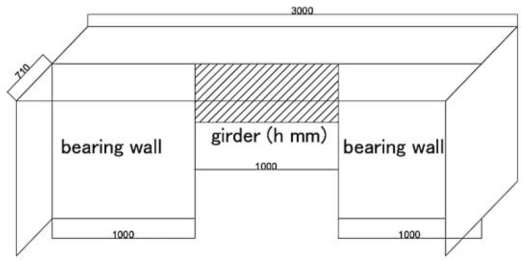

Fig.12 Model with girder

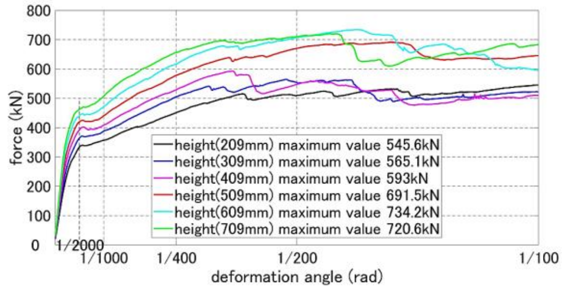

Fig.13 Comparison result with girders

structure. In view of the consideration, following two issues would be discussed in this part: (1), the tendency of strength affected by the height (h, mm) of girder up to 1/400 rad, but the results up to 1/100rad would be shown, (2), the effect of the height (h, mm) of girder on the fundamental expanding of effective length up to 1/100 rad. To discuss these two issues, other characteristics would be kept at the same value, just the height of the girder has been set up as 209mm, 309mm, 409mm, 509mm, 609mm, 709mm, respectively. The loading pattern is set up as the same as wall test mentioned in section 2.2.

Then the comparison of the strength for the whole wall element is presented in Fig.13: the models with girder height of 209mm, 309mm, 409mm, 509mm, 609mm and 709mm are showing the maximum value of strength of 548.1kN, 565.1kN, 593kN, 691.5kN, 734.2kN and 720.6kN, respectively. Overall, it can be known from the force-deformation curve that for the tendency of strength, the height of girder would bring effect: the strength of the whole H-type wall element with an opening in the bearing becomes larger as the height of the girder connecting the two bearing wall elements increases.

To show more details of these analyses, the distributions of cracking at 1/100 rad are shown in Fig.14 where the yellow element is showing softened concrete, the red element is showing post-softened concrete, the black line is showing the crack, the blue line is showing closed crack and the yellow line is showing sliding failure, from which it can be observed that:

In the cracking distribution in (a), (b), (c) of Fig.14 for height of girder of 209mm, 309mm, 409mm, it can be observed that the footing of the left bearing wall (tensile at the beginning) close to the opening, the connection part between the girder and the right bearing wall (compressive at the beginning) and the footing of the right bearing wall which is connected with out-of-plane wall are much easier to be cracked than

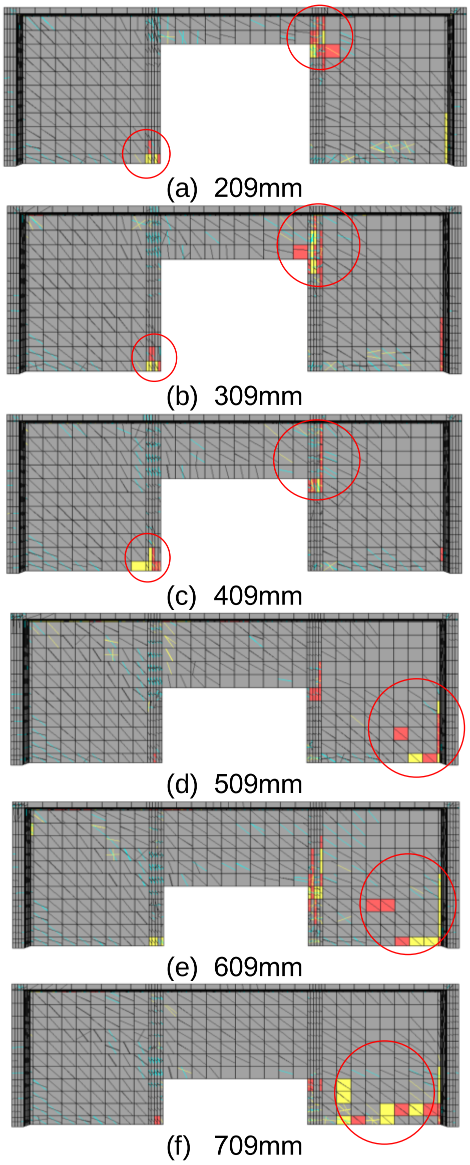

Fig.14 Cracking condition (1/100rad)

other parts. On the other hand, in the cracking distribution of (d), (e), (f) of Fig.14 for height of girder of 509mm, 609mm, 709mm, the footing of the right bearing wall (compressive at the beginning), the connection part between the bearing wall and the out-of-plane wall are observed to be much more cracked than other parts. Overall, two different tendencies of crack growth can be recognized: the footing of bearing wall which is carrying tensile force at the beginning and the connection part between the girder and the right bearing wall (compressive at the beginning) are observed less cracking, while the footing of the right bearing wall which is carrying compressive force at the beginning shows severer cracking as the height of girder increases. In other words, the bearing wall element (compressive at the beginning) carries stronger load as the height of girder increases.

Furthermore, to go to detail of these analyses, the minimum principal stress distributions at 1/100 rad are shown in Fig.15, the minimum principal stress distributions are showing similar tendency as shown in cracking condition above mentioned: the bearing wall

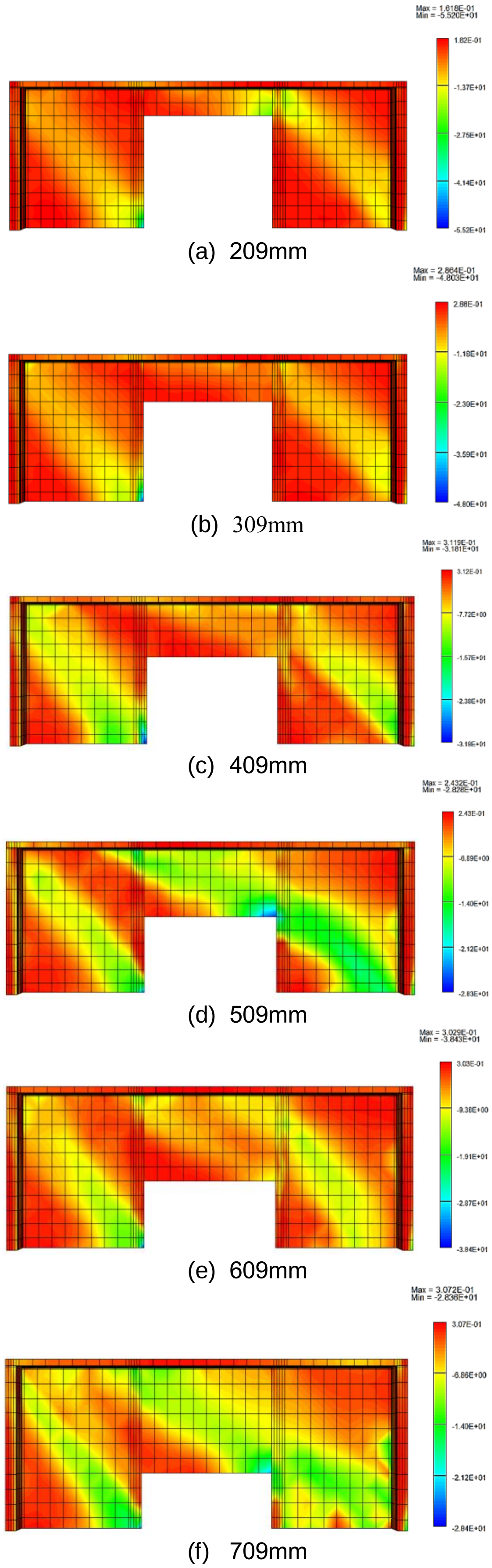

Fig.15 Minimum principal stress condition (1/100 rad and unit of stress is N/mm^2)

element (compressive at the beginning) carries stronger compressive load as the height of girder increasing.

Based on that the results are showing different tendency, the effective length of out-of-plane wall which is obtained from calculating method as described in Fig.1 in section 1 would be discussed separately for models with height of girder of 209mm, 309mm, 409mm and models with height of girder of 509mm, 609mm, 709mm. To show a full result of effective length, the calculation up to 1/67 rad are shown in following figures. For the models with height of girder of 209mm, 309mm, 409mm, as the height of girder increases, a uniform variation law cannot be defined at tensile side in Fig.16, while the effective length at compressive side is observed to be almost the same as Fig.17. On the other hand, For the models with height of girder of 509mm, 609mm, 709mm,, as the height of girder increases, a uniform variation law cannot be defined for the effective length at tensile side as Fig.18, while for the effective length at the compressive side, the critical point corresponding to all length effective region can be observed later as Fig.19.

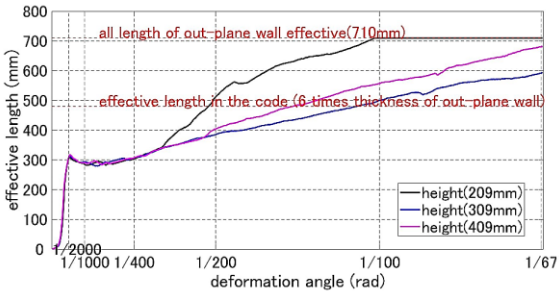

Fig.16 Effective length on tensile side

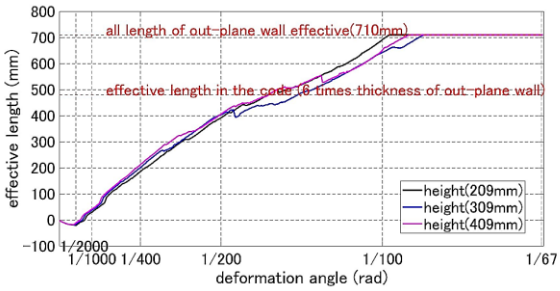

Fig.17 Effective length on compressive side

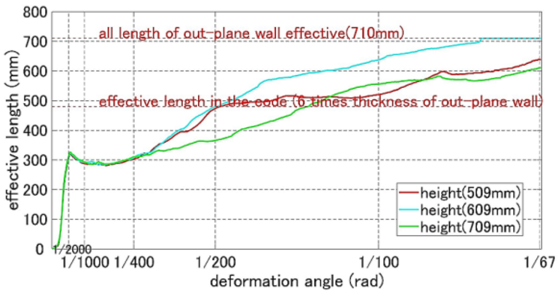

Fig.18 Effective length on tensile side

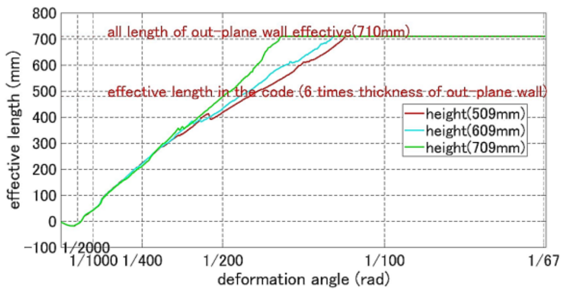

Fig.19 Effective length on compressive side

5. CONCLUSIONS

(1) The FEM analysis applied in this work is demonstrated as a reliable method for simulation of WRC structure limited within a small deformation while the modelling concept needs further research for large deformation.
(2) The strength of this H-type wall element with an opening in the bearing becomes larger as the height of the girder increases.
(3) Fundamental relationship has been observed for the effective length of out-of-plane wall with height of girder. However, a clear variation law cannot be established, which means it needs more detailed discussion in the further research.

ACKNOWLEDGEMENT

The authors acknowledge the support of Teshigawara laboratory from Nagoya University for providing wall test data and a very helpful discussion.

REFERENCES

[1] 日本建築学会編：壁式鉄筋コンクリート造設計・計算規準・同解説，pp．287，2015．12
[2] 佐々木智也，斎藤大樹，楠浩一：曲げ降伏する耐力壁の協力幅に関する実験的研究（その１：実験概要と実験結果・考察）,日本建築学会大会学術講演梗概集（東海），巻：2012 ページ：ROMBUNNO.23465.
[3] 平成 28 年度建築基準整備促進事業M４長期優良住宅における鉄筋コンクリート壁式構造の損傷防止性能の評価の合理化に関する検討.
[4] 長沼一洋，山口恒雄：面内せん断応力下におけるテンションスティフニング特性のモデル化，日本建築学会大会学術講演梗概集，構造II，pp.649-650,1990.10.
[5] 長沼一洋：三軸圧縮下のコンクリートの応力～ひずみ関係，日本建築学会構造系論文集，第 474 号，pp.163-170,1995.8.
[6] 長沼一洋，大久保雅章：繰返し応力下における鉄筋コンクリート板の解析モデル，第 536 号，pp.135-142, 2000.10.
[7] Elmorsi, M., Kianoush, M.R. and Tso, W.K. : Modeling bond-slip deformations in reinforced concrete beam-column joints, Canadian Journal of Civil Engineering, Vol.27, pp.490-505, 2000